PRECETRON—A PRINCIPLE FOR OBTAINING PION-PION AND MUON-MUON COLLISIONS*, **

ROBERT MACEK AND BOGDAN MAGLIC

Department of Physics
University of Pennsylvania, USA.

The construction of „pion factories" [1, 2, 3, 4] gives rise to the question of how far are we from observing real $\pi\pi$ and $\mu\mu$ collisions. Czonka and Sessler[6] have previously discussed the possible use of CERN intersecting storage ring for $\pi-P$ and $\pi-\pi$ scattering. The purpose of this note is to sketch the characteristics of a particular pion storage device and to estimate bounds for certain machine parameters needed to produce reasonable $\pi\pi$ and $\mu\mu$ collision rates. We call this device the „precetron" because the colliding orbits are constantly precessing.

A device for pion-pion collisions in the mass region of ρ meson has been proposed and its parameters calculated. It operates on the following idea: over 10^{13} π^+ and π^- in the momentum range P_π=310—555 MeV/c are produced by a short burst of 6×10^{15} protons of 800 MeV incident onto a metal target placed in the center of a 400 Kgauss (pulsed) magnetic field, extending over a radius of $R\simeq5$ cm and shaped to contain ~100 turns of pions. Pion orbits are circles tangential to the target; π^+ and π^- orbits precess in opposite directions, the locii of their centers being circles of radius $r\simeq{}^1/_2R$ whose origin is at the target. The $\pi^+-\pi^-$ collisions of interest take place in the peripheral region of this „magnetic pot", where the crossing angles of the intersecting precessing orbits are smallest. This orbit-precession device has a large momentum acceptance of pions, $\Delta p/p\simeq50\%$ and large angular acceptance, 0° to 180° in horizontal and $\pm10°$ in vertical plane, in contrast to a conventional storage

* Supported in part by the United States Atomic Energy Commission

** Доклад не зачитывался

ring which would require well-defined momentum and small angular divergence in order to have the pions captured.

Single particle orbits have been calculated to first order; they show the precessing character of the orbits and the stability of the free oscillation densities in the colliding region—an outer shell of thickness ηR—have been calculated as a function of η; number of protons/sec, N; magnetic field, B; proton pulse length, g, in units of pion laboratory lifetime (which is $\sim 10^{-7}$ sec); number of proton pulses/sec, b; and other parameters, eq. (28). The π-π collision rate is proportional to N^2B^3 and inversely proportional to bg^2 i. e. the poorer the duty cycle of the proton accelerator, the higher the rate. If a proton linac with g=b=1 can be made with the same average power as the Los Alamos Meson Factory (but with 600,000 times poorer duty cycle), there will be about 20,000 π-π collisions/hour. However, this b=g=1 regime can be also accomplished without changing the machine parameters, by storing the proton beam in a storage ring for $\sim$ 1 sec and dumping it onto the precetron target in one turn.

All backward scattered pions from $\pi^+\pi^- \rightarrow \pi^+\pi^-$, which represent $\sim$ 50% of the collisons, will leave the magnetic pot because of the change of the sign of the $\vec{v}\times\vec{B}$ force; their momenta will be measured outside and their directions after scattering reconstructed, to obtain the π-π effective mass of the collision (no knowledge of the crossing angles and energies before collision is needed to obtain the effective mass).

After several pion life-times, the muons from the decaying pions will be orbiting in similar precessing orbits and similar collision rates will be obtained.

I. DESCRIPTION OF THE „PRECETRON"

A. The setup

We consider the following setup: a solid metal target is placed in the center of a high magnetic field which is shaped to contain at least 100 turns of pions of momentum in the range P_π=310—550 MeV/c (T_π=200—430 MeV). We assume a magnetic field of 400 kG (probably a pulsed one) which gives a radius 3.3 cm for the pion orbit of an average energy T_π=300 MeV (P_π=415 MeV/c).

A proton beam is incident onto the target which is$\sim$2 cm thick in the beam direction and narrow ($\sim$0.2 cm). For the purpose of a simplified discussion we show in Fig. 1 the first turn for π^+ and π^- of one energy emitted at 30° to proton beam; this leads to four orbits. As we show later, these orbits precess about the z axis as indicated by the dashed arrow. There will be a similar family of orbits for each angle of pion emission.

In addition to pions, particles such as protons, deuterons and other light nuclei will also be produced and captured in the magnetic field.

Later on, after one pion lifetime, leptons will be present in the mixture too. We shall refer to this early mixture of positive and negative orbits of various hadrons with different crossing angles and momenta as the **hadron jumble**, in contrast to the **lepton jumble** that will be orbiting later.

We believe that a pulsed, iron-free field capable of containing the jumble can be produced by an appropriate coil configuration, and that a gap could be made about the midplane to allow exit of reaction products. Such a „magnetic pot" could be accomplished by a pair of coils with the current in both in the same direction (See Fig. 2), or by a more refined combination containing two pairs of coils of different radii and current[5]. This point is covered in Appendix I.

We have investigated the single particle orbits in a weak focusing field approximately given by $B_z = B_0 \left(1 - k \frac{r^2}{R^2}\right)$ where k is small, of order 0.1, and R is a radius which contains the „pot"; details are presented in Appendix I. These calculations indicate that, to first order, the radial and vertical oscillations are stable and that the orbits precess about the z axis, with a precession frequency $k'/4$ times the orbital frequency where $k' = k\left(\frac{2a}{R}\right)^2$ and a is the radius of orbit. Precessing single particle orbits for π^+ and π^- are shown in Fig. 3. For a uniform proton spill comparable or longer than the precession period we will have a uniform azimuthal distribution of orbit centers. In a shell near the outer envelope of the particle trajectory in Fig. 3, the particle is effectively providing a counter-clockwise current of say π^+'s. The π^- of the same momentum will move in the opposite direction and, in the outer shell, will be on a direct collision course with π^+ so that the crossing angle is approximately zero. The shell thickness can be a reasonable fraction of the orbit radius without containing large crossing angles. The particle density calculations are given in Appendix II.

The advantages of the above device over that of a more conventional storage ring lies with its large acceptance. Both the solid angle and momentum bit can be large. Production angles from zero to 180° are all captured. The vertical angle of emission with respect to the midplane is limited by the vertical acceptance and vertical oscillations, but, as shown in Appendix I, vertical angles of ± 0.15 radians are reasonable and lead to a solid angle acceptance of the order of 1 or 2 sr. In addition, the high field of this device confines the particles to a small volume and thereby increases the particle density.

Identification of $\pi^+\pi^-$ Collision Products From The Hadron Jumble

Les us consider the reaction

$$\pi^+ + \pi^- \rightarrow \pi^+ + \pi^- \qquad (1)$$

In P-wave scattering (rho meson), the angular distribution is strongly

peaked forward and backward equally. The π's scattered forward are unlikely to leave the pot since they will tend to be recaptured in quasi-stable orbits. However, the **backward scattered pions** will be immediately kicked out of the field by the change of sign of the $\vec{v}\times\vec{B}$ force. Particles scattered more or less in the direction of the major component of the field will also exit. Thus, a reasonable fraction, of order 1/2 of the collisions, will be detectable.

The concurrent reaction

$$\pi^+ + \pi^- \rightarrow \pi^0 + \pi^0 \qquad (2)$$

is obviously easier to detect regardless of the production angle. However, it can occur only from $l=0$. This excludes the P-wave (ρ meson) whose cross section is believed to be dominant by an order of magnitude over the non-resonant (l=even) cross section.

The products of the π-P scattering will come out of the pot in a similar way; the discrimination of pions from protons can be done in a standard way.

The calibration of the system could be done by using the π-P resonance and p-p scattering to map the proton current.

The effective mass of the pion-pion or pion-proton pair is measured by the magnetic analysis of their momenta outside the pot, with conventional wide gap magnets surrounding it. The invariant quanity $M^2_{\pi^+\pi^-} = (E_+ + E_-)^2 - (\vec{p}_+ + \vec{p}_-)^2$ is independent of the energies and crossing angles of π^+ and π^- before the collision. The directions and momenta have to be known only **after** the collision. The knowledge of the magnetic field topography is thus the only requirement necessary to reconstruct the collision vertex and to obtain the reaction energy, M_{+-}. Inelastic collisions are assumed to be negligible. Should there be a contribution from the G-parity violating process (electromagnetic) $\pi^+\pi^- \rightarrow \pi^+\pi^-\pi^\circ$, it could be detected by $\gamma\gamma$ conversion outside the pot. If two additional pions are produced ($\pi^+\pi^- \rightarrow \pi^+\pi^-\pi^\circ\pi^\circ$ or $2\pi^+ 2\pi^-$), of which only two charged pions are measured, the kinematic constraints can eliminate many possible misinterpretations of the event as an elastic one since. the sum of the energies of two pions in this case should lie in the limits $400 < T_+ + T_- < 800$ MeV; if two pions are missing, it will be observed in the limits $100 < T_+ + T_- < 500$ MeV.

II REACTION RATE

To estimate the π-π reaction rate in the hadron jumble and to study the important factors, we consider a simplified model with the following features, some of which will be modified later for a more precise calculation:

a) A point target;

b) A uniform particle distribution in the vertical (z) direction;
c) A uniform momentum distribution over the region of interest;
d) A π-production angular distribution which is isotropic to 45° then zero to 180°, also $\pi^-/\pi^+=x=1/4.5$;

e) We will only consider interactions from the region with orbit diameters from $\eta_l R$ to the maximum diameter, R. We will assume that the crossing angles are approximately zero in this region.

f) We will assume that the particle density is uniform in the region of interest. Later we will calculate using the actual particle density.

A. Basic formulae

In Fig. 4 we show schematically the region of interest which is the outer shell from $\eta_l R$ to R. Also shown are typical π orbits which reach the shell from which we accept interactions. In this shell the π's are moving mainly along the circumferences of circles whose centers are at the target. In the shell the π's effectively become two currents of opposite charge moving in opposite directions around the target.

If the π's spent all of their time in circular beams moving in opposite directions with 100% overlap and zero crossing angles, the instantaneous interaction rate dI/dt would be

$$\frac{dI}{dt}=2\sigma\beta_{12}c\frac{n_+n_-}{V} \tag{3}$$

where: $\sigma=\pi$-π cross section

n_+, n_-=the total number of π^+ and π^- particles, respectively which are functions of time.

β_{12} =the $\pi^+\pi^-$ relative velocity,

c =speed of light,

V =volume of the interaction region,

$$V=\pi R^2(1-\eta_l^2)\Delta Z\simeq 2\pi\bar{R}A, \tag{4}$$

where $\bar{R}$ is mean radius in the shell, A is the cross-sectional area of shell, and ΔZ is the vertical extension of the beam.

We can apply (3) to our problem by replacing n_+ and n_- by $n_+\bar{f}$ and $n_-\bar{f}$ where $\bar{f}$ is the average fraction of the time a π is in the outer shell. This is no more than saying that number of π's in the shell is the total number of π's times the probability that the π is in the shell.

For the orbit in Figure 4, f is the ratio of the arc length S to the total perimeter of the orbit, i. e.,

$$f(a)=\frac{S(a)}{2\pi a} \tag{5}$$

and

$$\bar{f}=\int_{\eta_l R/2}^{R/2} f(a)g(a)da, \tag{6}$$

where g(a) is the distribution of orbit radii (uniform) corresponding to the assumed momentum distribution.

From a simple consideration of this geometry in Fig. 4 we see that

$$S(a)=4a\cos^{-1}\frac{\eta R}{2a} \tag{7}$$

or

$$f(a)=\frac{2}{\pi}\cos^{-1}\frac{\eta R}{2a} \tag{7}$$

It should also be noted that $\pi f(a)$ is the maximum crossing angle for two orbits of radius a, intersecting inside the shell. For the intersection shown at r, the crossing angle α is

$$\alpha=2\cos^{-1}\frac{r}{2a}. \tag{8}$$

In general, two orbits of radii a_1 and a_2, intersecting at r have a crossing angle of

$$\alpha=\cos^{-1}\frac{r}{2a_1}+\cos^{-1}\frac{r}{2a_2} \tag{9}$$

Using (7) for f we obtain for $\bar{f}$

$$\bar{f}=\frac{2}{\pi}\int_{R\eta}^{R}\cos^{-1}\frac{MR}{X}\frac{dx}{R(1-M)}$$

$$=\frac{2}{\pi}\frac{\eta}{1-\eta}\left[\frac{1}{\eta}\cos^{-1}\eta-\log\left(\frac{1+\sqrt{1-\eta^2}}{\eta}\right)\right] \tag{10}$$

We are now ready to apply (3) to our problem with the result (using $N_-=kN_+$)

$$\frac{dI}{dt}=\frac{2\sigma\beta_{12}cn^2{}_+\chi\,\bar{f}^2}{\pi R^2\Delta Z(1-\eta^2)} \tag{11}$$

Let us replace R by an expression involving $\bar{R}$, the average orbit diameter. For the simple model under consideration

$$\bar{R}=R\frac{(1+\eta)}{2} \tag{12}$$

Finally,

$$\frac{dI}{dt}=\frac{2\sigma\beta_{12}cn^2{}_+\chi}{\pi\bar{R}^2\Delta z}K \tag{13}$$

where

$$K=\bar{f}^2(\eta)\cdot\left(\frac{1+\eta}{2}\right)^2\frac{1}{(1-\eta^2)} \tag{14}$$

is a function of η alone. For $\eta=1/2$ we have $\bar{f}(1/2)=0.49$ and $K=0.18$.

In Appendix II we derive a similar formula for this same model except that we calculate the actual particle densities D_+, D_- as functions of position. The rate is obtained from

$$\frac{dI}{dt}=\int_{\text{shell}} 2\sigma\beta_{12}cD_+D_-d(\text{vol}) \tag{15}$$

The result is formula (13) with a different expression for K (η_i) given by eqs. (74). Here we obtain K=0.25 for $\eta_i=1/2$.

In Appendix II we also calculate the case where the momentum distribution is peaked about the average value and for a shape closely approximating π production data. Once again formula (13) is obtained but with a different expression for K(η_i). In this case K=0.47 for $\eta_i=1/2$.

B. Time-Dependence for Decaying Particles

Let us calculate n(t) during and after a uniform proton burst. Figure 5 graphically depicts the situation. We assume that it will be too difficult to run with detectors turned on during the proton spill so that detectors will be turned on at the end of it.

When the protons are hitting the target (detectors **off**), the pion intensity builds up according to

$$n(t)=\alpha\tau(1-e^{-t/\tau}) \tag{16}$$

where τ is the laboratory life-time of the pion,

$$\tau=\gamma\tau_0, \tag{17}$$

and α = instantaneous π production rate which is proportional to the proton current, dN/dt;

$$\alpha=f\frac{dN}{dt}. \tag{18}$$

Here, N is the number of protons and f is the fraction of protons „transformed" into pions which are captured in the magnetic pot. The fraction f is given by

$$\int\frac{\delta^2\sigma}{\delta\Omega\delta P}d\Omega dP\frac{T}{A}N_0 \tag{19}$$

where T=target length, A=184 for tungsten and τ is the π life time in the laboratory, $\tau=\tau_\pi^{LAB}=\gamma\tau_0$.

Protons stop hitting the target after a time Δt and the detectors are switched **on**. The we have

$$n(t)=\alpha\tau(1-e^{-\Delta t/\tau})e^{-(t-\Delta t)\tau} \tag{20}$$

where Δt is the length of the proton burst and t anytime after the beginning of the burst. We shall now compute the number of interactions, I, produced from this burst while detectors are on:

$$I=\int_{\Delta t}^{\infty}\frac{dI}{dt}(t)dt=\frac{2K\ \sigma\beta_{12}c}{\pi\ \Delta zR^2}\int_{\Delta t}^{\infty}n_-(t)n_+(t)dt, \tag{21}$$

from which we obtain

$$I=[\tau^3(1-e^{-\Delta t/\tau})^2\alpha^2_+]\varkappa\frac{K\sigma\beta_{12}}{\pi\Delta z\bar{R}^2}, \tag{22}$$

where $\alpha_-=\varkappa\alpha_+=\varkappa\alpha$, and $\varkappa=\pi^-/\pi^+$ ratio which is~1/4,5 for 15° emission from 800 MeV protons on Beryllium.

Eq. (22) gives the number of interections per burst. The interaction rate per sec, $\bar{I}$ is then I times the number of bursts per second, b, so that

$$\bar{I}=\sigma\varkappa\alpha^2\tau^3\beta_{12}c(1-e^{-\Delta t/\tau})^2\frac{K}{\pi\Delta z\bar{R}^2}b \tag{23}$$

Equation (22) was derived on the assumption that all pion losses are due to the natural pion decay only. As will be discussed below, the effective pion lifetime, τ_π^{eff} will be shorter. Equation (22) is still valid by replacing $\tau_\pi^{LAB}\to\tau_\pi^{eff}$, where

$$\tau_\pi^{eff}=\phi\tau_\pi^{LAB}=\phi\bar{\gamma}_\pi\tau_0, \text{ and } \phi<1 \tag{24}$$

General features of the jumble are more easily seen by writing α, instead in equation (18), as

$$\alpha=\frac{fN}{b\Delta t} \tag{25}$$

where N=average number of protons on target/sec. Further we can express the burst length Δt as a fraction of π lab life time:

$$\Delta t=g\tau_\pi^{eff}=g\phi\gamma\tau_0, \tag{26}$$

where g is the ratio between the burst length and the effective pion lifetime.

Finally from eq. (65) we can replace Δz by

$$\Delta z\cong\frac{S\bar{R}}{\sqrt{k/2}}; \tag{27}$$

where S is the maximum accepted vertical slope (taken to be of order ~0.15). Making substitutions (25–27) we obtain:

$$\bar{I}\cong\frac{\sigma K\varkappa\ \bar{k}\beta_{12}c\phi\bar{\gamma}_\pi\tau_0f^2\bar{N}^2}{\pi S\bar{R}^3\sqrt{2}}\left(\frac{1-e^{-g}}{g}\right)^2\frac{1}{b}. \tag{28a}$$

One can replace the pion orbit diameter, $\bar{R}$, by

$$\bar{R}=2\bar{r}=\frac{2\bar{P}}{0.3B}=\frac{2\bar{\gamma}_\pi\bar{\beta}_\pi m_\pi}{0.3B} \tag{29}$$

where $\bar{P}$ is in MeV/c, B in kG, r in cm and obtain:

$$\bar{I}=\frac{2.4\times10^{-3}\sigma K\varkappa\sqrt{\bar{k}}\beta_{12}cB^3\phi\tau_0f^2\bar{N}^2}{\pi S\bar{\gamma}_\pi^2\bar{\beta}_\pi^3M_\pi^3}\left(\frac{1-e^{-g}}{g}\right)^2\frac{1}{b} \tag{28b}$$

In equations (28a, b) the quantities are:
σ=$\pi\pi$ total cross section ($\sim 10^{-25}$cm^2),
K=eqs. (14), (74), (80),
$\varkappa$=π^-/π^+ ratio,
k=eq. (39),
β_{12}=π-π relative velocity,
c=velocity of light,
B=magnetic field (kilogauss),
ϕ=eq. (24),
τ_0=natural $\pi^\pm$ lifetime,
$\bar{N}$=average number of protons/sec on target,
g=eq. (26),
b=number of bursts/sec,
S=maximum accepted vertical slope,
M_π=$\pi^\pm$ mass,
$\bar{\beta}_\pi$=average π velocity,
$\bar{\gamma}_\pi$=average value of E_π/m_π,

From equation (28) we see, within the limit of this model, that for a fixed number of protons per/sec, $\bar{N}$, **the luminosity is best for the poorest duty cycle**. L is maximum when the term

$$\frac{1}{b}\left(\frac{1-e^{-g}}{g}\right)^2 \qquad (30)$$

has a maximum.
The ratio in parenthesis has a broad maximum for a narrow burst, i. e., as $g \to 0$ Eq. (30)$\to 1/b$. The number of bursts, b, for a given average proton intensity should be as small as possible, hence the duty cycle, which can be written as

$$\text{Duty Cycle} = bg\gamma\phi\tau_0, \qquad (31)$$

hould be as small as possible. In other words, a high **instantaneous** intensity of π's produced per second, is desired. It is obviously more advantageous to produce them in one burst of the order of, or shorter than the effective pion lifetime.

The luminosity is directly proportional to the third power of the containing magnetic field, B, for a given momentum and fixed acceptance. The highest π-π collision rates will be near the target because D_+ is largest there, but we have excluded this region because of two complications:

a) Large crossing angles which can be anywhere from 0 to 180°;

b) Interactions of pions with target.

Hence results computed from eq. (28) will be a **lower limit** on the rate.

C. EFFECTIVE PION LIFETIME

Pions will be lost from the hadron jumble not only by their natural decay but by their multiple traversals through the target. To estimate the

amount of material seen we use the following simplified model. All orbits are tangent to the z axis, which goes through the center of the target. Due to the vertical free oscillations, the orbits uniformly populate, (approximately) the vertical aperture. Thus, the average length, $\bar{S}$, of target traversed per orbit is

$$\bar{S}=\frac{w}{\Delta z}\bar{S}_{proj}, \tag{32}$$

where Δz is the vertical aperture (4 cm), w the width of the target (0.2 cm) and $\bar{S}_{proj}$ the average projected length traversed if all orbits are projected onto the z=0 plane (see Fig. 6). For a target of thickness 2 cm in the beam direction and 0.2 cm wide square cross section we obtain $\bar{S}_{proj}=0.5$ cm based on a calculation using the above model. Thus $\bar{S}=0.025$ cm.

The traversal losses arise from three factors:

a) Energy degradation. For the tungsten target described above 300 MeV π's will lose 100 MeV in 180 turns. This should be compared to the 125 turns they make in one laboratory lifetime.

b) Multiple scattering. This will cause small losses. The total multiple scattering in 125 turns is 6°, while our vertical angular acceptance is around $\pm$ 10°.

c) Nuclear interaction. The interaction length in tungsten is 7.8 cm while 180 turns corresponds to 4.4 cm of traversal. From this we can see that collision losses will be as important as decay losses in limiting luminosity. Collision losses can be represented by a collision lifetime, τ_c, so that the effective τ_π is

$$\tau^{eff}=\frac{\tau_c\tau_\pi^{LAB}}{\tau_c+\tau_\pi^{LAB}} \tag{33}$$

Traversal of 7.8 cm corresponds to 310 turns or about 2.5 natural lifetimes. Thus, $\tau_c\approx 2.5\tau_\pi^{LAB}$ and

$$\tau_\pi^{eff}=0.7\tau_\pi^{LAB} \tag{34}$$

or $\phi=0.7$

A NUMERICAL EXAMPLE

We shall now compute the pion-pion collision rates using Eq. (28). The number of proton bursts/sec, b, and the burst length in units of pion lab life-time, g, will be kept general.

Other beam parameters, including the average beam power, will be taken from the LAMPF proposal[1].

According to LAMPF studies (p. 29 of ref. 1), a 1 mA average proton beam (6×10^{15} p/s) of 800 MeV incident upon 18 grams/cm^2 Be target will yield, at 15°, 1.1×10^{10} π^+/sec (with $T_\pi=300$ MeV, in a channel with the momentum and solid angle acceptances $\Delta p=6.7\%$, $\Delta\Omega=3\times10^{-3}$ at 43 ft from the production point (the decay length is 74.6 ft). From this we

compute the pion yield per 1 mA of protons, Y, per gram/cm² Be per st/MeV/c to be

$$Y=1.28\times10^{10}\pi^+/\text{sec/gr/cm}^2\text{/Be/sr/MeV/c} \tag{35}$$

Scaling this by $(A_{Be}/A_w)^{1/3}$ to obtain a tungsten yield gives

$$Y=4.7\times10^{9}\pi^+/\text{sec/gr/cm}^2\text{w/sr/MeV/c/1mA/protons}$$

Assuming that the π-production cross section is constant out to 45° and then drops abruptly to zero, we obtain an effective solid angle of 0.45 sr. We take a momentum bit of $\Delta P/P=.5$ full width. Other numbers are 38 gr of tungsten, $\phi=0.7$, $\tau_0=2.8\times10^{-8}$, $\varkappa=1/4.5$, $\gamma=3$, $\beta_{12}\simeq1.0$, $\bar{R}=6.6$ cm and $\Delta z=4$ cm, or $S=0.15$, and $\beta\pi\simeq1.0$. With these numbers, the luminosity from Eq. (28) becomes

$$L=4.3\times10^{29}\frac{1}{b}\left(\frac{1-e^{-g}}{g}\right)^2 \text{ per cm}^2 \text{ per hour,} \tag{36}$$

or, using the cross section for $\pi^+\pi^-$ at the ρ-resonance peak ($T_{\pi+}=T_{\pi-}=240$ MeV), $\sigma=10^{-25}$ cm², the rate becomes

$$\bar{R}=4.3\times10^{4}\frac{1}{b}\left(\frac{1-e^{-g}}{g}\right)^2 \text{ interactions/hour.} \tag{37}$$

For the presently planned structure of the beam at LAMPF (120 pulses, 500 μsec long, where $b=120$, $g=5\times10^3$) we obtain one π-π collision every $.7\times10^5$ hour $\simeq10$ year. However, with $b=g=1$, which means that all the protons hit the target in **one** burst of duration 0.1 μsec, we get 17000 π-π collisions per hour. With $b=1$, $g=0.1$ (10 ns burst) the rate becomes 39,000/hour, as shown in Table I. Both these last cases require between 6×10^5 and 6×10^6 **poorer duty cycle** with the same average power.

To find an optimum solution for the maximum reaction rate at a reasonable instantaneous power, let us discuss equation (36). The duty cycle is proportional to the product bg, which we will maximize in order to ease the instantaneous power requirement. For large g, $g>10$, the function

$$G'=\left(\frac{1-e^{-g}}{g}\right)^2 \tag{38}$$

is a very small number, $G^2<10^{-2}$. For $g<10$, G^2 rises fast to unity as $g\to0$. The smallest g to choose is right after the fastest rate of change of G^2, i. e., after $\delta G^2/\delta g=\text{max}$. This happens for $0<g<0.1$; there, G^2 has values in the region 0.4—0.95, respectively. We do not gain by going below $g=0.1$. Referring to Table I, we see that with 10,000 bursts of $\Delta t=0.1$ μsec ($b=10^4$, $g=1$ or 60 times poorer duty cycle) one obtains 2 π-π interactions per hour.

In conclusion, one can have anywhere between **2 and 39,000 π-π interactions per hour** if one can make a 1 mA proton machine with the

same average beam power but whose **duty cycle** is between 60 and 600,000 times **poorer** (instantaneous power 60 to 600,000 times **higher**) than the planned duty cycle of LAMPF (6%).

E. Proton Storage Ring

An alternate solution to decreasing the linac's duty cycle has been suggested by D. Nagel (Priv. Comm.): the protons from a number of linac pulses are collected into a storage ring and then dumped in one short pulse. With this procedure one could obtain $b=g\approx 1$ if protons can be stored in a ring of radius r=300 cm and switched out in one turn ($\sim 10^{-7}$ sec). This would yield about 5 π-π collisions per storage ring pulse. Proton injection into storage ring may be facilitated by using the 100 microamp H^--beam at LAMPF. The 800 MeV H^--ions can be converted to 800 MeV protons with very thin stripping foils.

F. Limitations

We enumerate and comment on some important approximations of our calculations as well as some practical limitations of our „precetron" model:

1. Collective phenomenon such as space charge effects, beam-beam interactions, etc. have been neglected in our treatment of orbits. Only single particle orbits were computed and then only to first order. A study obtaining more exact single particle orbits and of collective effects are the next step.

2. A 400 Kg field in the volume required is yet to be accomplished. However it has been achieved in a 5/8" bore[7].

3. The 0.2 cm diameter, 2 cm long tungstan target in our numerical example must dissipate around 50 KW of power. At LAMPF a 1 cm diameter 10 cm long graphite target has been stably operated while dissipating 62 KW. At incipient burn-out this target was receiving 94 KW[8].

4. Radiation damage to the coils of this device may be a problem but it is a common problem to the thick target facilities of meson factories.

III. MUON-MUON COLLISIONS

A. THE LEPTON JUMBLE

The solid metal target in the middle of the „magnetic pot", will gradually (within a few effective π lifetimes) remove all undecayed hadrons by stopping them or by scattering them out. Only the muons from the pion decay and few electrons from the mu-decay will stay in orbit. The orbits will eventually pull away the target, as shown in Fig. 7B. The mechanism by which the lepton orbits get detached from the target is the following: muons from π decay are generally emitted at

an angle different from 0° with the pion direction (Fig. 7A). While the parent pion was heading toward the target at which it was created (Liouville's theorem), the muon direction is generally different and thus will **avoid** the target. The exception is when the decay takes place too close the target to escape it. A large fraction of the muons will miss the target and continue orbiting in a new phase space. The muons that hit the target will continue traversing it until all their energy is lost.

B. MUON-MUON LUMINOSITY AND REACTION RATE

Because of their 100-times longer life-time than that of π's, Eq. (28) is approximately valid for the muon rate too (daughter much longer living than parent). The only difference is that 100 times **lower** instantaneous rates (higher duty cycle) are needed, because now g=1 means 10 μsec pulse, rather than 0.1 μsec which was the case for π's,and the luminosity goes up by 100.

In terms of the muon lifetime, the planned time structure of the LAMPF beam is b=120, g=50, for which Eq. (28) gives a luminosity of 10^{24}/cm^2/hr. But the μ-μ cross section is $\sim 10^3 - 10^4$ times smaller than that for the strongly interacting pions, so that it gives one μ-μ scattering every 10^5 hours. On the other hand, with g = 1(10 μsec pulses) and b≅100, one gets **20 μ-μ collisions per hour,** with the duty cycle 60 times poorer than the one planned for LAMPF.

The advantages of the proton storage ring, discussed above, apply equally well to the muon case.

Table 1

Pion-Pion Luminosity and Interaction Rate

Pion-Pion luminosity and interaction rates are shown as function of proton burst length, g(in units of effective π life time) and b, the number of burst/sec. These are calculated using eq. (36) and (37). Only the outer shell contribution (η=1/2) are included hence their results are lower limits.

Burst length g in units of eff. π life-time	b burst/sec	Luminosity L cm^{-2}/hr	Collision rate σ L $\pi+\pi\to\pi+\pi$ interactions hour
5×10^3	120	1.4×10^{30}	1.4×10^{-5}
10	1	4.3×10^{27}	430
50	10	1.7×10^{25}	1.7
1	1	1.7×10^{29}	17,000
1	10	1.7×10^{28}	1 700
1	100	1.7×10^{27}	170
1	1,000	1.7×10^{26}	17
0.1	1	3.9×10^{29}	39,000
0.1	10	3.9×10^{28}	3,900
0.1	100	3.9×10^{27}	390
0.1	1,000	3.9×10^{26}	39
0.01	1	4.3×10^{29}	43,000
0.01	100	4.3×10^{27}	430
0.1	10,000	3.9×10^{25}	3.9
1	10,000	1.7×10^{25}	1.7

APPENDİX I

ORBIT CALCULATIONS

An exact solution of Maxwells equations (in cylindrical coordinates) which posseses focussing properties is

$$B_\theta = 0 \tag{a}$$

$$B_r = \frac{-2k}{R^2} B_o rz \tag{b}$$ (39)

$$B_z = B_o\left[1 - \frac{kr^2}{R^2} + \frac{2kz^2}{R^2}\right] \tag{c}$$

where k and R are constants. The constant R is introduced to make k dimensionless and will be taken as a radius characteristic of the dimension of the magnetic „pot." In the main text we use $\bar{r}_0$ the average pion orbit diameter as this characteristic radius.

Such a field, for small k. can be approximately achieved around the midpoint of two identical coils of radius a separated by a distance 2d, d≠a. The first few terms in an expansion of B_z in terms of z/a and r/a are[9]

$$B_z = \frac{\mu I}{a} \sin\alpha \left[P_1^1(\cos\alpha) + P_3^1(\cos\alpha)\left(\frac{2z^2 - r^2}{2a^2}\right) + P_5^1(\cos\alpha)\frac{(8z^4 - 24z^2r^2 + 3r^4)}{8a^4}\right] + \cdots, \tag{40}$$

where P^1_n are the associated Legendre functions and tan α=a/d. The corresponding expansion for B_r is

$$B_r = -\left(\frac{\mu I}{a}\sin\alpha\right)\left[P_3^1(\cos\alpha) + \frac{(4z^2 - 3r^2)}{2a^2} P_5^1(\cos\alpha)\right]\left(\frac{rz}{a^2}\right) \tag{41}$$

By using two sets of coils each of different radii, separations, and currents, it is possible to choose these parameters to obtain any desired value for the ratio of coefficients of second order to zeroth order terms and at the same time make the fourth order term vanish. Thus, departures from Eq. (40) comes in only at 6th order and higher. Clearly, by a suitable arrangement of sets of coils of varying radii and separations, one can approximate (39) as closely as is needed.

The field given by (39) can be obtained from a scaler potential, φ, given by

$$\phi(r, z) = B_o z\left(1 - \frac{kr^2}{R^2} + \frac{2kz^2}{3R^2}\right) \tag{42}$$

The equipotential surfaces of (42) give rise to the following family of curves in θ=const. planes:

$$r^2 = \frac{R^2}{k}\left(\frac{\phi}{B_o z} - \frac{2kz}{3R^2} - 1\right) \tag{43}$$

These are shown graphically in Fig. 7 for a typical case k=0.1 and R=1. One could also achieve (39) by suitably shaped iron pole tips in a magnet.

The equations of motion for $B_\theta=0$ in cylindrical coordinates are

$$m\ddot{r}=mv\dot{\theta}^2+(e/c)r\dot{\theta}\,B_z, \qquad (a)$$

$$\frac{d}{dt}(mr^2\dot{\theta})=\frac{er}{c}(\dot{z}\,B_r-rB_z), \qquad (b) \quad (44)$$

$$m\ddot{z}=\frac{er}{c}\dot{\theta}\,B_r \qquad (c)$$

where $m=m_o\sqrt{1-\beta^2}$ and $\beta=v/c=$constant for static fields. Eq. (44b) can be integrated once to give using the initial $r(0)=0$

$$\dot{\theta}=\frac{\omega_o}{2}\left(1-\frac{kV^2}{2R^2}+\frac{2kz^2}{R^2}\right) \qquad (45)$$

where $\omega_0=-eB_o/cm$.

Substituing (45) for $\dot{\theta}$ yields the following coupled equations for r and z:

$$\ddot{z}=-\omega_0^2\frac{k}{R^2}\cdot r^2z\left(1-\frac{kr^2}{2R^2}+\frac{2kz^2}{R^2}\right), \qquad (a)$$

$$\ddot{r}=-\frac{r\omega_0^2}{4}\left[1-\frac{2kr^2}{R^2}+\frac{4kz^2}{R^2}+\frac{k^2r^2}{R^4}\left(\frac{3}{4}-4z^2+4z^4\right)\right], \qquad (b) \quad (46)$$

We shall take initial conditions as

$$\begin{aligned} &r(0)=z(0)=\theta(0)=0,\\ &\dot{r}(0)=v_r\neq 0,\\ &\dot{z}(0)=v_z\neq 0. \end{aligned} \qquad (48)$$

For k=0, the motion is simple, i. e.,

$$\begin{aligned} \theta&=\frac{\omega_0 t}{2},\\ r_o&=2a\sin\theta,\\ \dot{z}_o&=z(0)t,\\ \omega_0&=\frac{v_r}{a},\\ a&=\frac{v_r}{\omega_0}. \end{aligned} \qquad (47)$$

These are helical orbits whose motion in z=constant planes are circular orbits. If we now consider k and z^2/R^2 as small quantities and expand (45) and (46), keeping only lowest order terms, we have

$$\ddot{z}=-\omega_0^2\frac{k^2}{R^2}r^2z \qquad (a)$$

$$\ddot{r} = -\frac{r\omega_0^2}{4}\left(1-\frac{2kr^2}{R^2}\right) \qquad \text{(b)} \quad (49)$$

$$\dot{\theta} = \frac{\omega_0}{2}\left(1-\frac{kr^2}{2R^2}\right) \qquad \text{(c)}$$

Eq. (49 b) has solutions in terms of Jacobian elliptic functions.

$$\mathrm{Sn}\left(\frac{\omega_0 t}{2\sqrt{m^2+1}}\middle|\, m^2\right), \tag{50}$$

where

$$m^2 = \frac{1-\sqrt{1-4k'}}{2k'} - 1. \tag{51}$$

$$k' = \left(\frac{2a}{R}\right)_k^2$$

This can be seen by integrating (49 b) once using the substitution $\dot{r} = P$ and obtaining

$$\dot{r}^2 = v_r^2 - \frac{\omega_0^2}{2}\left(\frac{r^2}{2} - k\frac{r^4}{2R^4}\right) \tag{52}$$

Using $v_r^2 = \omega_0^2 a^2$, (52) becomes

$$\dot{r} = \omega_0 a\sqrt{1-\left(\frac{r}{2a}\right)^2 + k'\left(\frac{r}{2a}\right)^4}. \tag{53}$$

Integrating (53) once leads to

$$\frac{\omega_0 t}{2\sqrt{m^2+1}} = \int_0^u \frac{du}{\sqrt{(1-u^2)(1-m^2u^2)}}, \tag{54}$$

where

$$u = \frac{r}{2a\sqrt{m^2+1}}$$

and

$$m^2 = \frac{1-\sqrt{1-4k'}}{2k'} - 1. \tag{55}$$

Eq. (54) is a standart elliptical integral defining the Sn function[10].

Therefore, the solution of (49 b) is

$$r = 2a\sqrt{m^2+1}\ \mathrm{Sn}\left(\frac{\omega_0 t}{2\sqrt{m^2+1}}\middle|\, m^2\right) \tag{56}$$

An expansion of (56) to first order in k′ yields[11]

$$r = (2a)\left(1+\frac{9}{16}k'\right)\left(\sin\alpha t + \frac{k'}{16}\sin 3\alpha t\right), \tag{57}$$

where $\alpha = \frac{\omega_0}{2}\left(1-\frac{3k'}{4}\right)$. (58)

Using Eq. (57) for r, we obtain, to first order in k′, the following relationship:

$$\theta=\int_0^t \dot{\theta}\,dt=\frac{\omega_0}{2}[(1-k'/4)t+(k'/8\alpha)\sin 2\alpha t] \tag{59}$$

We can use (59) to eliminate t from (57) and obtain r (θ). Carrying this out to first order in k′ results in

$$r=2a(1+k'/2)\sin\theta(1-k'/2) \tag{60}$$

From (60) it is clear that the orbits precess about the z axis with a period $4/k'$ times the orbital period.

The solution (57) can nov be inserted into Eq. (46a) to obtain an equation for the z motion. Thus,

$$\ddot{z}=-\omega_0^2 k' z \sin^2\alpha t$$

or

$$\ddot{z}+\frac{\omega_0^2}{2}k'(1-\cos 2\alpha t)t=0 \tag{61}$$

Eq. (61) is in the standard form for Mathieu's equation and possesses a Floquet solution, which for small k is[12]

$$Z(t)=\frac{\dot{z}(0)}{\sqrt{r}}\sqrt{\left(\frac{2}{k'}\right)}\frac{a}{(1-k'/2)}\left(\sin\frac{\omega_0}{2}\sqrt{2k'}t\right)\left(1-\frac{k'}{2}\cos 2\alpha t\right) \tag{62}$$

Thus, the vertical oscillations are stable with amplitude S, given by

$$S=S_0\sqrt{\frac{2}{k'}}\,\frac{a}{(1-k'/2)}, \tag{63}$$

where S_0 is $\dot{z}(0)/v_r$, the initial slope in a vertical plane containing the z axis. Let $h=\Delta z/2$ be the vertical half aperture, then the maximum acceptable slope is

$$S_m=\frac{h}{a}\sqrt{\left(\frac{k'}{2}\right)}(1-k'/2)$$

$$=\frac{\Delta z}{R}\sqrt{k/2}\left(1-\left(\frac{2a}{R}\right)^2 k\right)\simeq\frac{\Delta z}{R}\sqrt{k/2}. \tag{64}$$

For $\Delta z=4$ cm, $R=6.6$ cm, and $k=0.1$ we obtain $S_m\simeq 0.15$ radian

In the main text we express Δz in terms of S_m and R where we use for R, the characteristic radius of the pot, the average pion orbit diameter denoted $\bar{R}$; hence

$$\Delta z\simeq S_m\bar{R}\sqrt{2/k} \tag{65}$$

The calculations reported here have been made only to first order in k and $(z/R)^2$. It is possible that higher order terms may couple vertical and radial oscillation in such a way as to be unstable for even small k and $(z/R)^2$. To investigate this we will, in the future numerically intergrate the coupled eqs. (46a) and (46b).

APPENDIX II

PARTICLE DENSITY CALCULATIONS

We wish to calculate the particle density ρ, for a δ function orbit diameter x, distribution. We assume a uniform distribution for z and θ_0, where θ_0 is the angle of the orbit center in cylindrical coordinates. Clearly, ρ is a function of r only; hence we will set $\theta=0$. As shown in Fig. 9a, two orbits pass through each given point (r, θ).
The density ρ is defined by

$$\rho(r)dV=\rho(r)\,rdrd\theta dz=\text{number of particles in dV}$$

$$=2\left(\frac{N_T}{2\pi\Delta z}d\theta_0 dz\right)\left(\frac{dS}{2\pi a}\right) \tag{66}$$

The factor 2 is present because of the two orbits at $\pm\theta_0$.
The first factor in parenthesis is the number of orbits around θ_0 which pasts through dV as shown in Fig. 9b; and the second factor is the fraction of each orbit in dV. N_T is the total number of particles considered. Now $r=2a\cos\theta_0$. and

$$ds=\frac{rd\theta}{\cos\theta_0}=2ad\theta$$

Hence,

$$\rho(r)dV=\frac{N_T}{\pi^2(\Delta z)}d\theta_0 dz d\theta=\rho(r)rdrd\theta dz$$

and

$$\rho(r)=\frac{N_T}{\pi^2(\Delta z)r}\frac{\partial(\theta_0,\theta,z)}{\partial(r,\theta,z)}=\frac{N_T}{\pi^2(\Delta z)r\sqrt{4a^2-r^2}},$$

where the Jacobian is

$$\left|\frac{dr}{d\theta_0}\right|^{-1}=\frac{1}{\sqrt{4a^2-r^2}}.$$

Letting $x=2a$, we have

$$\rho(r,x)=\frac{N_T}{\pi^2\Delta z}\cdot\frac{1}{\sqrt{x^2-r^2}}\cdot\frac{1}{r} \tag{67}$$

The density ρ, is normalized to N_T, the total number of particles, as the integral below shows:

$$\int_{pot}\rho(r)rdrd\theta dz=N_T.$$

If we now take an x distribution f(x), corresponding to some momentum distribution, then the π^+ particle density $\vec{D_+(r)}$ is given by

$$D_+(r,\theta,z)=N_+\int_r^R\frac{f(x)dx}{\pi^2(\Delta z)r\sqrt{x^2-r^2}}=D_+(r), \tag{68}$$

where N_+ is the total number of orbiting π^+'s. The interaction rate dI/dt is then determined from

$$\frac{dI}{dt}=\int_{\substack{\text{vol. of}\\ \text{shell}}} 2\sigma D_+ D_- \beta_{12} c dV. \tag{69}$$

For a uniform x distribution in a shell from $\eta_l R$ to R we have

$$f(x)=\frac{1}{(1-\eta_l)R} \qquad \eta_l R \leq x \leq R \tag{70}$$

and D_+ becomes

$$D_+(r)=\frac{N_+}{1-\eta_l}\ \frac{1}{\pi^2 R(\Delta z) r}\ \mathrm{Sech}^{-1}\frac{r}{R}. \tag{71}$$

Using this in (69) yields

$$\frac{dI}{dt}=\frac{2\sigma\beta_{12}c\varkappa K}{\pi \bar{R}^2 \Delta z} N_+^2, \tag{72}$$

where

$$\bar{R}=\frac{R(1+\eta_l)}{2}, \tag{73}$$

$$K=\frac{(1+\eta_l)^2}{(1-\eta_l)^2 2\pi^2}\int_{\eta_l}^{1}\frac{dx}{x}(\mathrm{sech}^{-1}x)^2. \tag{74}$$

If we take $\eta_l=12$, $K\simeq 0.25$.

The actual π^+ momentum distribution is not uniform and will modify the results above. A convenient polynomial approximatiou for f(x) corresponding to the π^+ spectrum expected from 800 MeV protons[13] on tungsten is

$$f(x)=\frac{12}{R}\left(\frac{x}{R}\right)^3\left[1-\frac{x^2}{R^2}\right] \qquad 0\leq x\leq R. \tag{75}$$

R is the maximum diameter orbit. The distribution (75) yields an average value, $\bar{x}$ given by

$$\bar{x}=\bar{R}=0.69\,R \tag{76}$$

and, a variance σ_x of

$$\sigma_x=0.35\bar{R}=0.25\,R. \tag{77}$$

Using (75) we obtain D_+

$$D_+=\frac{8}{5\pi^2}\ \frac{N_+}{R(\Delta z)r}\left(1-\frac{r^2}{R^2}\right)^{\frac{3}{2}}\left(1+\frac{4r^2}{R^2}\right). \tag{78}$$

Computing dI/dt using (78) and (69) results in

$$\frac{dI}{dt}=\frac{2\sigma\beta_{12}c\varkappa K N_+^2}{\pi(\Delta z)\bar{R}^2}, \tag{79}$$

where

$$K=\frac{128}{25\pi^2}\,0.49\int_{\eta_l}^{1}\frac{dy}{y}(1-y^2)^3(1+4y^2)^2. \tag{80}$$

If $\eta_l=1/2$, then $K\simeq 0.47$.

Acknowledgements

We are particularly thankful to Kenneth Robinson for his most valuable explanations, discussions and important suggestions used in this study and to Stanley Livingston for his hospitality and discussions during the stay of one of us (P. M.) at Cambridge Electron Accelerator as visiting scientist.

We are indebted to Gerald O'Neill and to D. Nagel for their most useful discussions and encouraging attitudes to our idea of π-π collisions.

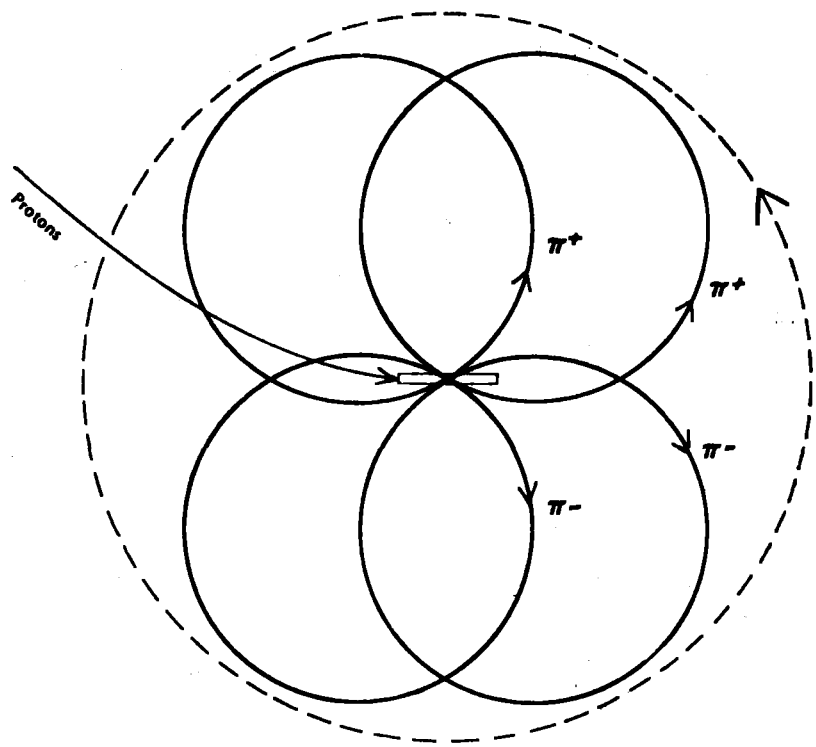

Fig. 1 First turn for + and − of median energy emitted at 30° to proton beam. The dashed line gives the direction of the π+ orbit precession. B is directed into the plane of the paper; it is centered at the target center and is shown in Fig. 2

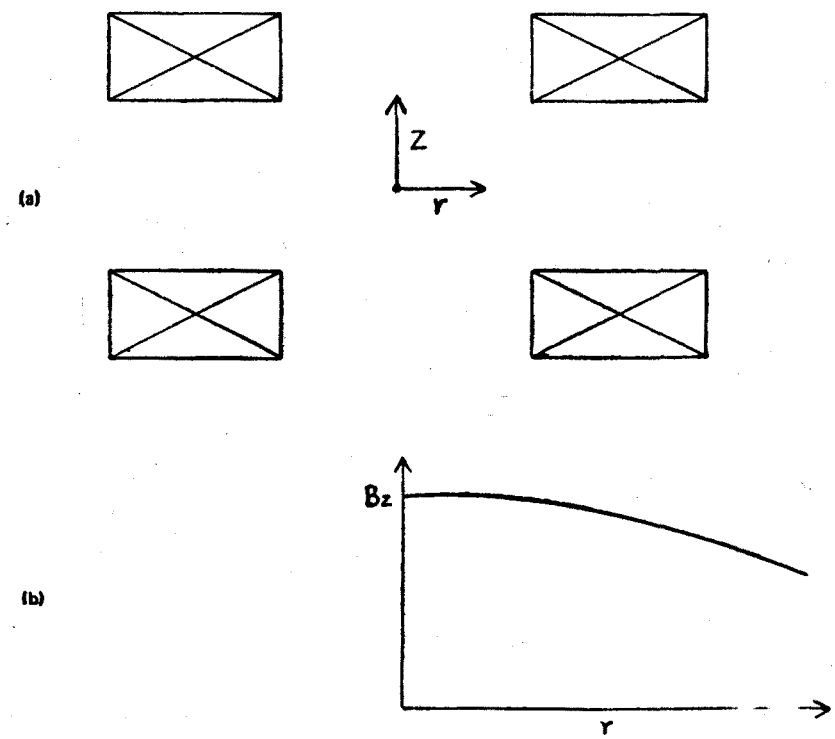

Fig. 2 (a) Possible coil configuration. For more omplex configuration see ref. (5).
(b) Major field component as function of r.

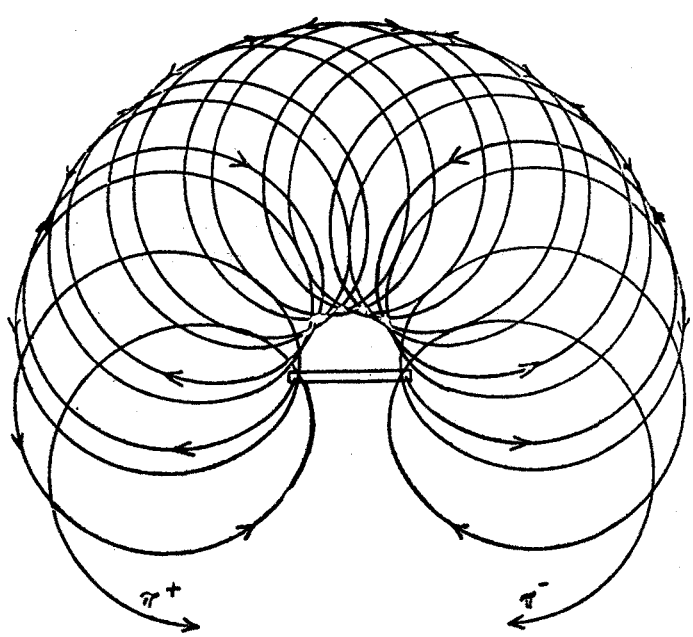

Fig. 3 Typical $\pi+$ and $\pi-$ colliding orbits of **one** momentum showing precession.

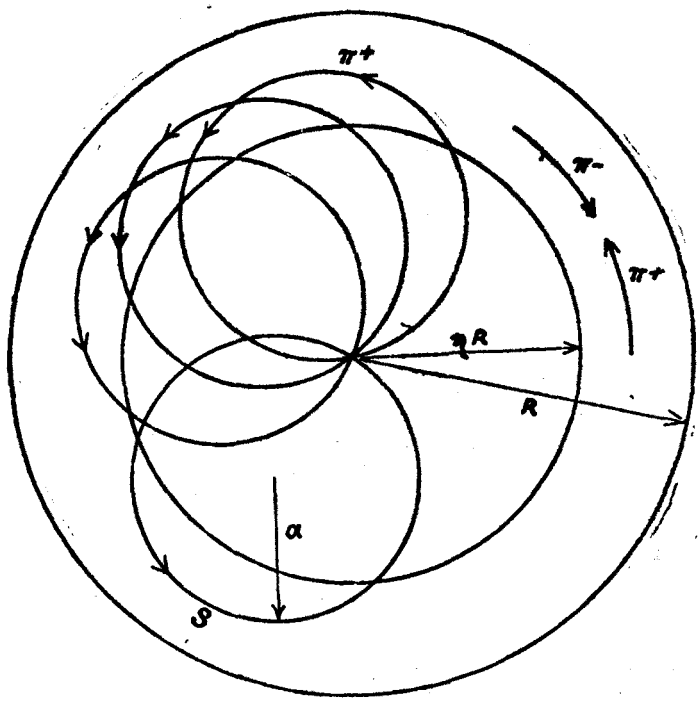

Fig. 4 Typical π+ orbits showing the shell from which the interactions are accepted.
The shell is the region of radii from ηR to R.

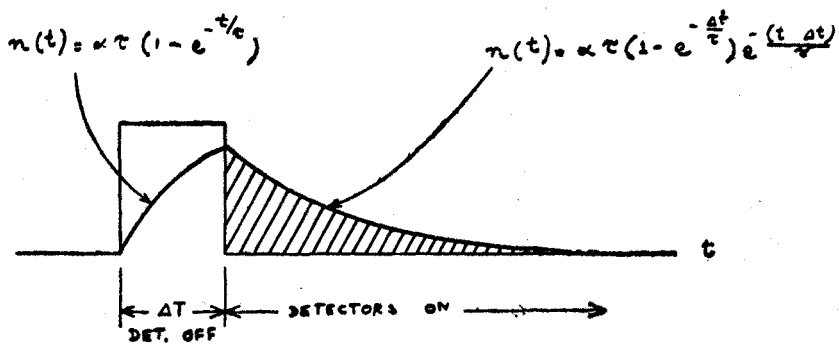

Fig. 5. Pion intensity as a function of time. ΔT=length of the proton spill onto the target inside the pot; τ=laboratory pion life-time.

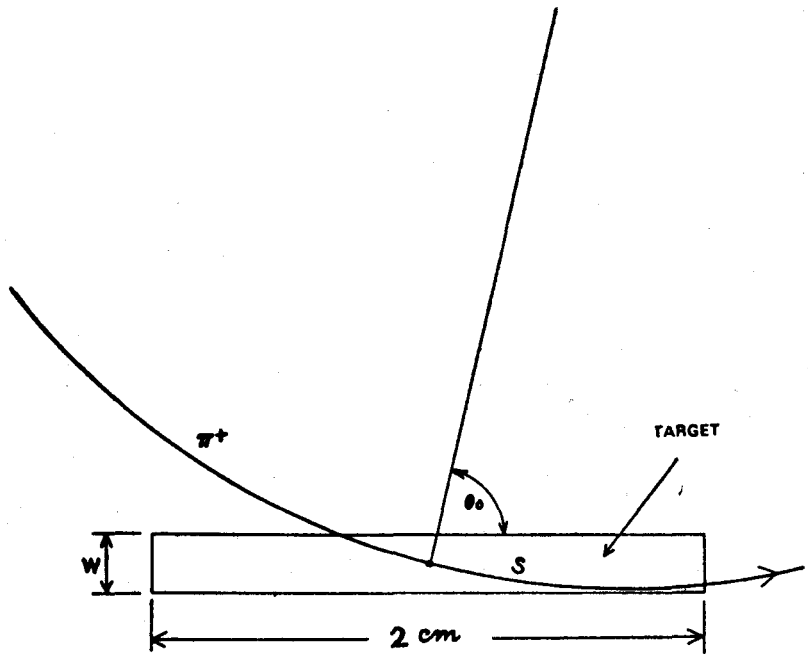

Fig. 6 Schematic showing amount of target material traver ed by π+ whose orbit lies in the midplane and whose orbit center lies on a line thru the target center which makes an angle of θ_0 with respe t to the target.

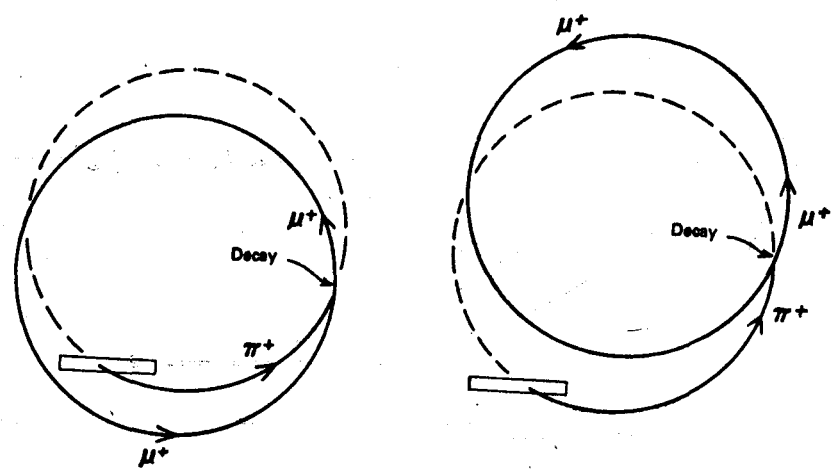

Fig. 7 (a) Two examples of π+ →μ+ decay which produce μ+ orbits which will never hit the target.

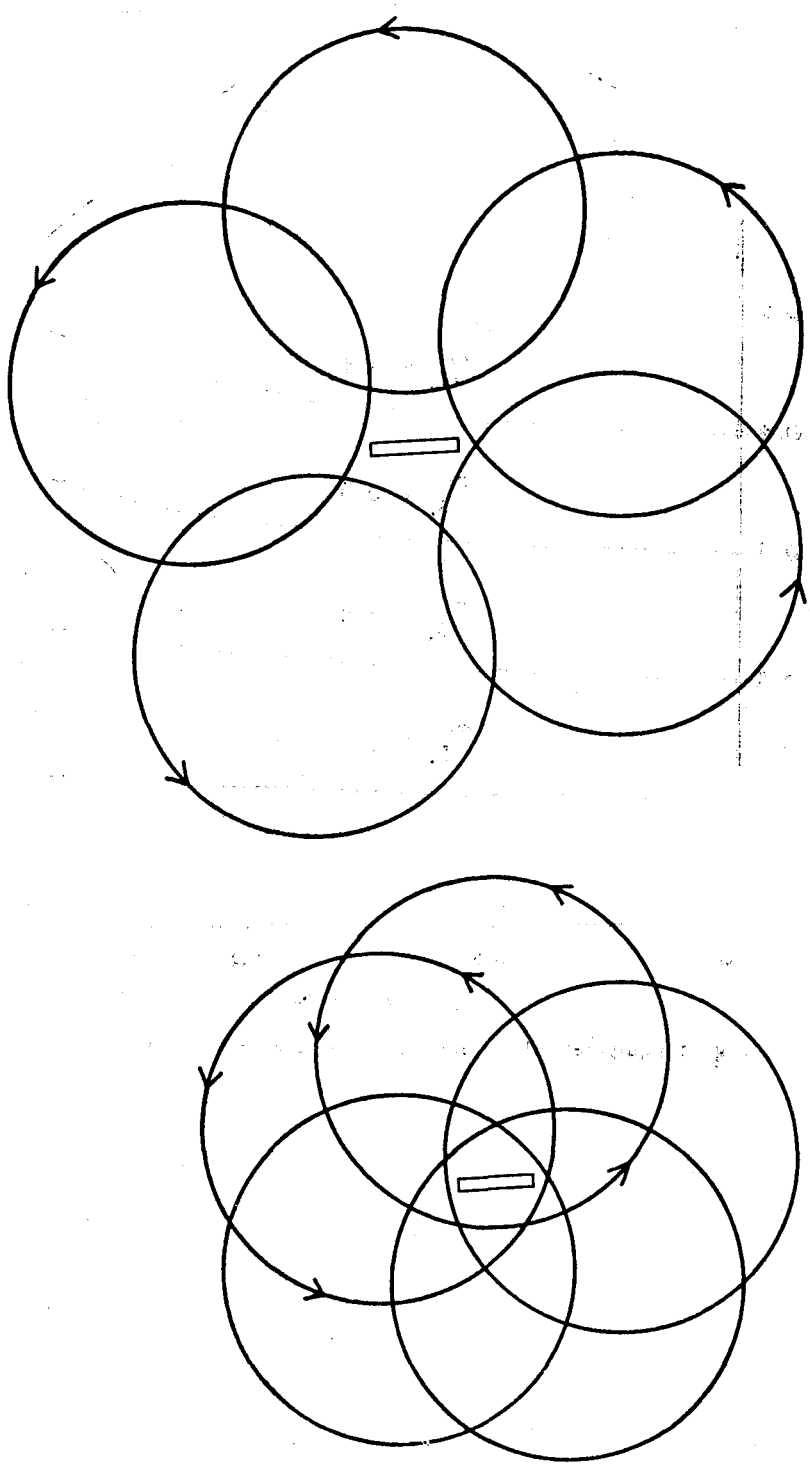

(b) Families of orbits correspondin~ to the two examples of decay in Fig. 7a

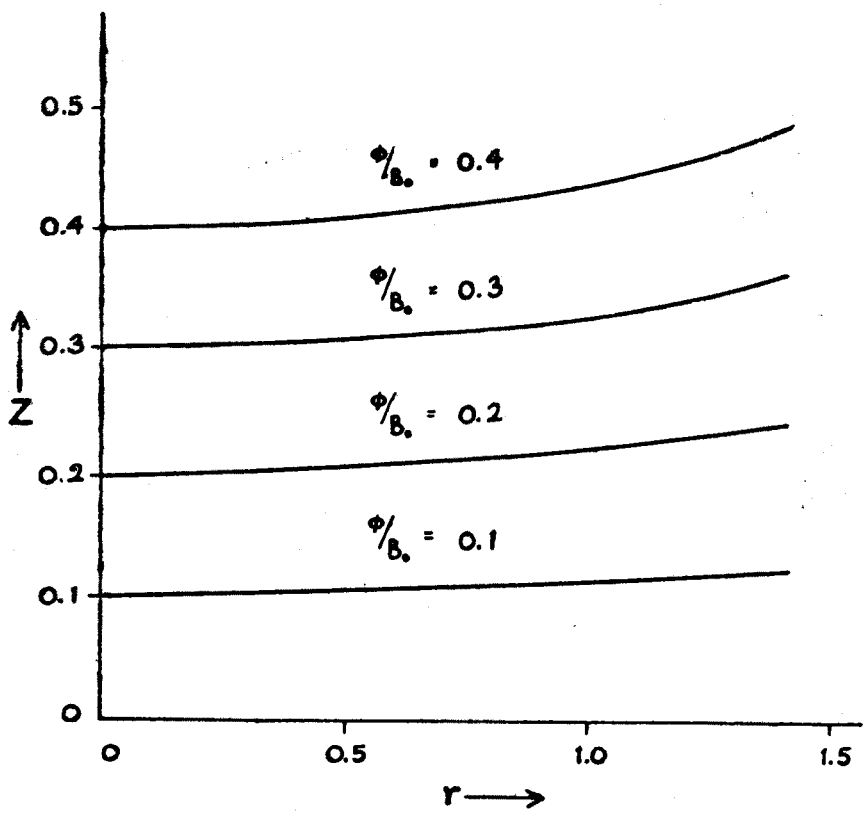

Fig. 8 Equipotential surfaces for the ase k=0.1 a d R=1.0.

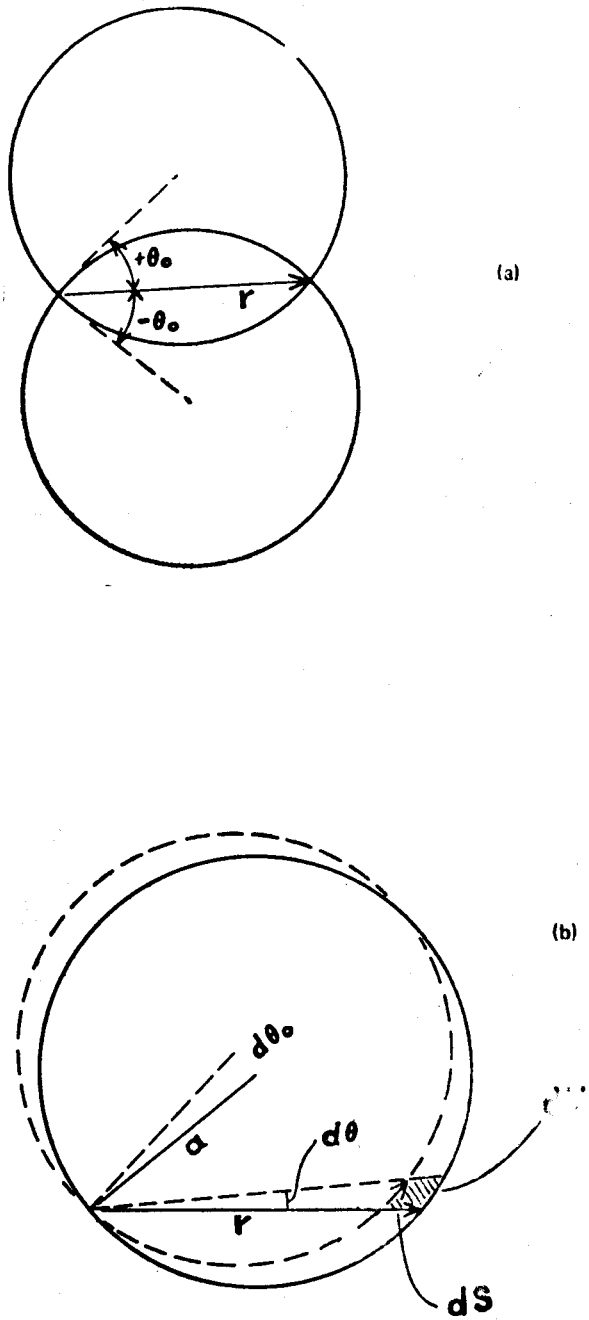

Fig. 9 (a) Two orbits at $\pm\theta_0$ passing thru point r.
(b) Orbits defining dV.

REFERENCES

1. Los Alamos High Flux Meson Facility (800 MeV), LASL Report 1964 L. Rosen, Meson Factories, Physics Today, December 1956, p. 21.
2. Isochronous Ring Cyclotron (580 MeV), Swiss Institute for Nuclear Research, Zurich.
3. Tri-University Meson Facility (500 MeV), Vancouver B. C.
4. Spiral Ridged Cyclotron (700 MeV), Dubna.
5. J. Applied Physics **21**, 1108 (1950); H. Kanter, Annalen der Physik **41**, 35 (1942); J. Oostens, **Revue De Circle Industrielle, Ecole Speciale, Univ. Louvin, Belgium,** p. 49 (1956)
6. ISR/CERN Report, PS/597/EEK; ISR-TH-167—29 1967).
7. S. Foner, Nat. Magnet Lab. MIT, private communication.
8. D. R. F. Cochran, **Procedings of the 2nd LAMPF Users Meeting,** 1969; LA—4087-MS, Page 23.
9. Smythe, **Static and Dynamic Electricity,** p. 274.
10. athews and Walker, **Mathematical Methods of Physics**. Chapts. 16 and 17
11. NBS, **ibid.**, p. 575, Eqn. 16. 23. 1 and p. 591.
12. Erdelyj, et al., **Higher Transcendental Functions,** Vol. 3 pp. 97 and 105.
13. Eq. (75) is a reasonable approximation to π^+ spectrum shown on page 35 of the proposal for the **Los Alamos High Flux Meson Facility** 1964